


Cite this: *Dalton Trans.*, 2023, **52**, 16591Received 15th October 2023,  
Accepted 31st October 2023

DOI: 10.1039/d3dt03416j

rsc.li/dalton

## A planar per-borylated digermene†

Xiongfei Zheng, Agamemnon E. Crumpton, Mathias A. Ellwanger and  
Simon Aldridge \*

A tetraboryl digermene synthesized by the reaction between a dianionic digermanide nucleophile and a boron halide electrophile is dimeric both in the solid state and in hydrocarbon solution. It features both a planar 'alkene-like' geometry for the  $\text{Ge}_2\text{B}_4$  core, and an exceptionally short  $\text{Ge}=\text{Ge}$  double bond. These structural features are consistent with the known electronic properties of the boryl group, and with lowest energy (*in silico*) fragmentation into two triplet bis(boryl)germylene fragments.

Carbenes and their heavier group 14 analogues (tetrylenes) have received considerable recent attention, not least because of their ability to activate small molecules such as  $\text{H}_2$ , CO and alkenes in 'transition-metal like' fashion.<sup>1,2</sup> The ambiphilic nature of two-coordinate systems of the type  $\text{EX}_2$  ( $\text{E} = \text{C-Pb}$ ), and the availability of frontier orbitals of both  $\sigma$  and  $\pi$  symmetry allow the possibility for synergistic interactions with small molecules which have both donor and acceptor properties.<sup>3</sup> As with d-block systems, the extent of such interactions is influenced significantly by the energies of the frontier orbitals, which in turn reflect factors such as the identity of the group 14 element E, the X-E-X angle, and the electronic properties of the X-substituents. X groups featuring highly electronegative donor atoms and/or strong  $\pi$ -donor capabilities tend to lead to a stabilised  $\sigma$  symmetry orbital (typically the HOMO), a destabilised  $\pi$  orbital (often the LUMO, or an orbital close to it), and consequently a wide HOMO-LUMO energy gap.<sup>3</sup> On the other hand, boryl substituents (*i.e.*  $\text{X} = \text{BR}_2$ ) offer the opposite scenario – namely a narrow HOMO-LUMO gap, brought about by the electropositive and non  $\pi$ -donor nature of the donor atom.<sup>4</sup> As such, boryl-substituted tetrylenes have shown unusually high levels of reactivity in the activation of molecules, being implicated in the first examples of both

silylenes and stannylenes to oxidatively add  $\text{H}_2$  (**I-Si** and **II-Sn**; Fig. 1).<sup>5,6</sup>

Steric factors are also important in tetrylene systems – not only in influencing the magnitude of the X-E-X angle, but also their tendency towards dimerization to give ditetrelenes,  $\text{X}_2\text{EEX}_2$ .<sup>7</sup> These heavier alkene analogues typically adopt *trans*- $\text{C}_{2h}$  skeletal geometries, which can formally be regarded as being constructed by the dimerization of two singlet  $\text{EX}_2$  fragments (which become increasingly stabilized with respect to the corresponding triplet state on descending group 14).<sup>8</sup>

Given the heightened reactivity shown by bis(boryl)-stannylene **II**, and the accessibility of digermavinylidene **III**,<sup>9</sup> we were interested here to explore strategies for the synthesis of the corresponding bis(boryl)germylene, **II-Ge** (Fig. 1). In the event, the combination of an energetically accessible triplet state for the  $\text{Ge}(\text{boryl})_2$  fragment, allied to steric limitations in the boryl groups available synthetically, led to the isolation of the corresponding (planar) tetraboryl-digermene.

While the germanium (and silicon) analogues of the heteroleptic (amido)(boryl)stannylene  $\text{Sn}\{\text{N}(\text{SiMe}_3)\text{Dipp}\}(\text{boryl})$  (**I-Sn**),

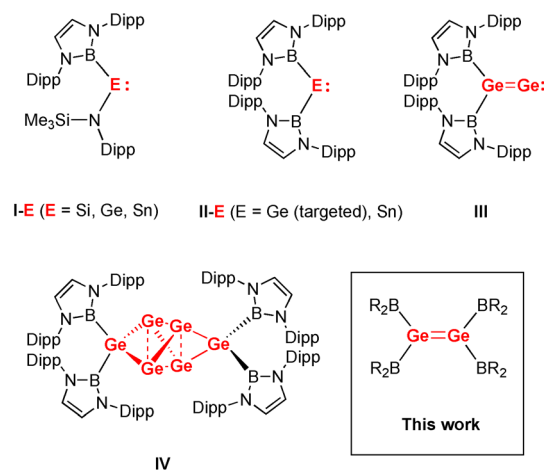


Fig. 1 Boryl-substituted tetrylene and related systems of relevance to the current study.

*Inorganic Chemistry Laboratory, Department of Chemistry, University of Oxford, South Parks Road, Oxford, OX1 3QR, UK. E-mail: simon.aldridge@chem.ox.ac.uk*

† Electronic supplementary information (ESI) available: Full synthetic/characterizing data, X-ray CIFs and details of calculations. CCDC 2300941–2300943. For ESI and crystallographic data in CIF or other electronic format see DOI: <https://doi.org/10.1039/d3dt03416j>



are readily accessible,<sup>5</sup> attempts to synthesize  $\text{Ge}(\text{boryl})_2$  (**II-Ge**) *via* reactions of  $\text{GeCl}_2 \cdot \text{L}$  (L = dioxane, NHC) or  $\text{Ge}\{\text{N}(\text{SiMe}_3)_2\}_2$  with two or more equivalents of  $(\text{boryl})\text{Li}(\text{thf})_2$ <sup>10</sup> proved unsuccessful in our hands (where  $\text{boryl} = -\text{B}(\text{NDippCH})_2$ ). In addition, the reaction of the hexa-germanium system  $\text{Ge}_6(\text{boryl})_4$  (**IV**)<sup>11</sup> with reducing agents such as  $\text{KC}_8$ , targeting  $\text{Ge}(\text{boryl})_2$  by liberation of the known tetrahedral cluster *nido*- $[\text{Ge}_4]^{4-}$ ,<sup>12</sup> also did not lead to the isolation of the desired germylene product. With this in mind, we turned our attention to an umpolung synthetic strategy, *via* the use of nucleophilic sources of the  $[(\text{boryl})\text{Ge}]^-$  fragment, with the idea of assembling a second Ge–B bond by reaction of  $\text{M}_2\text{Ge}_2(\text{boryl})_2$  (M = Group 1 metal)<sup>9</sup> with a boron-centred electrophile.

$\text{K}_2\text{Ge}_2(\text{boryl})_2$  (**1**) is available *via* the exhaustive reduction of  $(\text{boryl})\text{Ge}(\text{IPrMe})\text{Cl}$  using  $\text{KC}_8$ ,<sup>9</sup> and we sought to expand the range of nucleophilic group 1 metal digermanide derivatives by synthesizing a related lithium compound. However, rather than a reductive protocol starting from  $(\text{boryl})\text{Ge}(\text{IPrMe})\text{Cl}$ , the dilithium species  $\{(\text{IPrMe})\text{Li}\}_2\text{Ge}_2(\text{boryl})_2$  (**2**) is most conveniently prepared from **1** by a salt metathesis reaction with lithium iodide, in the presence of the carbene IPrMe (Scheme 1 and Fig. 2).<sup>‡</sup> **2** can be obtained *via* this route in *ca.* 30% yield after recrystallization from toluene/hexane. Its solid-state structure, determined by X-ray crystallography, is based around a  $\text{Ge}_2$  unit featuring two boryl groups arranged in 1,2-fashion (and *trans* to one another), with each germanium centre being additionally bound to a single lithium atom. Each lithium centre is also coordinated by a single NHC donor ( $d(\text{Li}-\text{C}) = 2.133(5) \text{ \AA}$ ), and engages in weaker contacts with two of the carbon atoms of a Dipp group associated with the boryl ligand attached to the other germanium centre ( $d(\text{Li} \cdots \text{C}) = 2.702(7), 2.743(7) \text{ \AA}$ ). In contrast to the solid-state structure of **1** (and related terphenyl-ligated systems) in which the alkali metal cation sits above the centre of the  $\text{Ge}_2$  unit and is further encapsulated by  $\pi$ -interactions with the flanking aryl rings,<sup>9,13</sup> the positioning of the lithium atoms in **2** suggests greater directionality in the Ge–Li interactions. The associated Ge–Li distances ( $2.541(7) \text{ \AA}$ ) are slightly greater than the sum

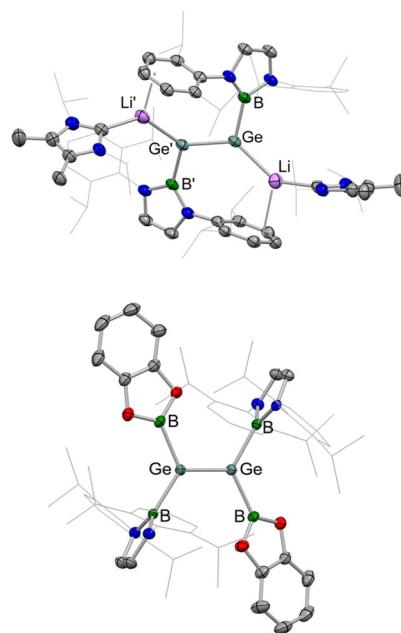
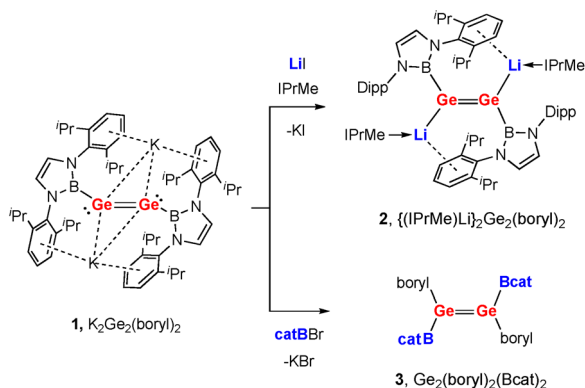


**Fig. 2** Molecular structures of (upper)  $\{(\text{IPrMe})\text{Li}\}_2\text{Ge}_2(\text{boryl})_2$  (as the pentane solvate,  $2 \cdot \text{C}_5\text{H}_{12}$ ) and (lower) of one of the (four) components of the asymmetric unit of  $\text{Ge}_2(\text{boryl})_2(\text{Bcat})_2$  (**3**) in the solid state as determined by X-ray crystallography. Hydrogen atoms and solvate molecules omitted, and certain carbon atoms depicted in wireframe format for clarity; thermal ellipsoids set at the 25% probability level. Key bond lengths ( $\text{\AA}$ ) and angles ( $^\circ$ ): (for **2**) Ge–Ge 2.3453(5), Ge–B 2.091(3), Ge–Li 2.541(7), Li–C<sub>NHC</sub> 2.133(5), Li–C<sub>aryl</sub> 2.702(7), 2.743(7), B–Ge–Ge–B 166.7(1); (for **3**) Ge–Ge 2.234(1), 2.235(1), 2.235(1), 2.238(1); Ge–B<sub>Bcat</sub> 2.022(3), 2.025(3), 2.026(3), 2.026(3), 2.028(3), 2.028(3), 2.031(3), 2.033(3), Ge–B<sub>boryl</sub> 2.023(2), 2.025(2), 2.025(3), 2.027(2), 2.027(2), 2.028(3), 2.028(3), 2.028(3); B–Ge–Ge–B 180.0(1), 177.3(1), 179.6(1), 180.0(1).

of the respective covalent radii ( $1.20 + 1.28 \text{ \AA}$ ),<sup>14</sup> and the geometry at each germanium centre defined by the proximal boron, germanium and lithium centres is trigonal planar ( $\Sigma(\text{angles at Ge}) = 358.8(3)^\circ$ ).

The straightforward substitution of the  $\text{K}^+$  cations in **1** by  $\text{Li}^+$  in the reaction with  $\text{LiI}/\text{IPrMe}$  led us to investigate its reactivity towards boron-based electrophiles, with the aim of generating a diborylgermylene. However, neither **1** or **2** reacts with  $(\text{boryl})\text{Br}$  to give a species of empirical composition  $\text{Ge}(\text{boryl})_2$  under any conditions examined – presumably due to the excessive steric demands of the boryl Dipp substituents and relatively low electrophilicity of  $(\text{boryl})\text{Br}$  enforced by the presence of two  $\alpha$ -amido  $\pi$  donors. With this in mind we turned to the less sterically demanding boron electrophile,  $\text{catBBR}$  (cat = 1,2- $\text{O}_2\text{C}_6\text{H}_4$ ) as has previously been employed by Cui in related silicon chemistry.<sup>15</sup> Reaction with **1** leads to clean conversion in *ca.* 65% yield (after recrystallization from pentane), to yield the unsymmetrical *trans*-1,2-tetraboryl digermene,  $\text{Ge}_2(\text{boryl})_2(\text{Bcat})_2$  (**3**; Scheme 1).<sup>‡</sup> **3** is characterized by two  $^{11}\text{B}$  signals at  $\delta_{\text{B}} = 28.9$  and  $43.6$  ppm, and its dimeric structure in the solid state, together with the relative arrangement of the two different sets of boryl ligands has been confirmed by X-ray crystallography (Fig. 2).



**Scheme 1** Synthesis of lithiated and borylated derivatives of  $\text{K}_2\text{Ge}_2(\text{boryl})_2$  (**1**) *via* metathesis processes with  $\text{LiI}/\text{IPrMe}$  and  $\text{CatBBR}$ , respectively. (IPrMe =  $\text{C}\{\text{N}(\text{Pr})\text{CMe}_2\}_2$ ).



The solid-state structure of **3** contains four molecules within the asymmetric unit, and reveals an exceptionally short Ge–Ge separation (2.234(1)–2.238(1) Å). This distance can be compared to 2.4 Å for the sum of the (single bond) covalent radii,<sup>14</sup> 2.347(2) Å for the digermene Ge<sub>2</sub>{CH(SiMe<sub>3</sub>)<sub>2</sub>}<sub>4</sub>,<sup>16</sup> and 2.285(1) Å for the digermene Ge<sub>2</sub>Ar<sup>Dipp</sup><sub>2</sub> (where Ar<sup>Dipp</sup> = 2,6-C<sub>6</sub>H<sub>3</sub>Dipp<sub>2</sub>).<sup>17</sup> Moreover, in contrast to the *trans*-bent structures observed for digermenes such as Ge<sub>2</sub>{CH(SiMe<sub>3</sub>)<sub>2</sub>}<sub>4</sub>, **3** adopts a planar geometry at each germanium centre ( $\Sigma$ (angles at germanium) = 358.2–360.0°) with an inter-planar angle (between the least-squares planes defined by the two GeB<sub>2</sub> units) in the range 0–4.8°.

The Ge–Ge distance measured for **3** (2.236 Å (mean)) is successively shorter than those determined for dilithium compound **2** (2.3453(5) Å) and dipotassium species **1** (2.392(1) Å).<sup>9</sup> Notwithstanding the predominantly non-bonding nature of the (*a*<sub>g</sub>, *n*<sub>+</sub>) HOMO in doubly reduced digermene species such as **1**,<sup>13</sup> this sequential shortening presumably reflects a reduction in the partial negative charge at each germanium centre on assimilation of the Li(NHC) and (particularly) the more covalently bound Bcat fragment. In a broader context, the ‘alkene-like’ form of **3** is reminiscent of the geometries determined for tetrasilyldigermenes, which also evidence near-planar structures with very small *trans*-bending and inter-planar angles.<sup>18</sup> The Ge=Ge distances measured for **3**, are however, even shorter than those measured for silyl-substituted systems, and are among the shortest measured for any digermene.<sup>19</sup>

Viewing **3** as having a geometric structure closer to a conventional alkene than the *trans* bent geometry typical of heavier group 14 E<sub>2</sub>R<sub>4</sub> species, implies that it can be formally constructed by combining two triplet (rather than singlet) germylene fragments. Dimerization *via* ‘conventional’  $\sigma$  and  $\pi$  bond formation rather than a two-way donor–acceptor interaction offers a rationale for the structural features observed for **3** and related silyl-substituted systems.<sup>7,8</sup> This in turn is consistent with the influence of the strongly electro-positive boryl (and silyl) substituents at germanium, which are known to lead to a small HOMO–LUMO energy gaps (and low-lying triplet states) for tetrylene systems of the type E(boryl)<sub>2</sub>. By means of comparison, singlet–triplet energy separations of –0.3, 17.9 and 39.2 kJ mol<sup>–1</sup> have previously been calculated

for the tetrylene systems E(boryl)<sub>2</sub> (where E = Si, Ge and Sn, respectively).<sup>5</sup>

With this in mind, we examined computationally the fragmentation of a range of digermenes, Ge<sub>2</sub>X<sub>4</sub>, into both singlet and triplet germylenes (GeX<sub>2</sub>) by ETS-NOCV methods (Table 1).§ In the cases of **3** and Ge<sub>2</sub>(SiMe<sub>2</sub><sup>t</sup>Bu)<sub>4</sub>,<sup>18b</sup> cleavage into triplet germylene fragments clearly represents the lowest energy fragmentation pathway (*e.g.*  $\Delta E_{\text{orb}} = +155.4$  vs. +299.2 kJ mol<sup>–1</sup> for **3**). On the other hand, the cleavage of Lappert’s tetraalkyl digermene is most easily accomplished to give singlet Ge{CH(SiMe<sub>3</sub>)<sub>2</sub>}<sub>2</sub> fragments ( $\Delta E_{\text{orb}} = +157.0$  vs. +142.6 kJ mol<sup>–1</sup>), consistent with the observed *trans* bent structure of the digermene.<sup>16</sup> Only in the case of the *trans* bent, but twisted system Ge<sub>2</sub>Trip<sub>3</sub>(SiPh<sub>3</sub>) (among the digermene systems examined),<sup>20</sup> were the two fragmentation pathways found to be of comparable energy ( $\Delta E_{\text{orb}} = +159.1$  and +160.5 kJ mol<sup>–1</sup>, respectively).

An alternative approach to probe the nature of the Ge=Ge bonds in planar and *trans*-bent cases (exemplified by **3** and Ge<sub>2</sub>{CH(SiMe<sub>3</sub>)<sub>2</sub>}<sub>4</sub>), involves the use of localised molecular orbitals (LMOs) to visualise the primary interactions between the two metal centres.<sup>§</sup> In the case of **3**, the LMOs which account for significant electron density at the bond critical point (BCP) and 1 Å above the BCP (Fig. 3) resemble classical  $\sigma$ - and  $\pi$ -type bonding orbitals. By contrast, in the case of Ge<sub>2</sub>{CH(SiMe<sub>3</sub>)<sub>2</sub>}<sub>4</sub>, two essentially equivalent LMOs each account for 48% of the electron density at the BCP (Fig. 4), and are of a form consistent with the ‘slipped’  $\pi$ -bond description, distorted in each case towards one of the two germanium centres.<sup>7,18</sup>

The speciation of **2** and **3** in hydrocarbon solution was also investigated. Most informatively, the UV-Vis spectrum of **2** in methylcyclohexane and **3** in pentane feature strong bands at 423 and 431 nm, respectively, *i.e.* similar to those measured for species containing Ge=Ge double bonds (*e.g.* 455 nm for [Ge(IDipp)]<sub>2</sub>,<sup>21</sup> and 434 nm for (boryl)Ge=Ge(IPrMe)(boryl)).<sup>9</sup> In the case of **3**, the assignment of the band at 431 nm is aided by the results of TD-DFT calculations. The S<sub>1</sub> absorption (2.932 eV, 423 nm) is predominantly due to a Ge=Ge  $\pi$  to  $\pi^*$  transition, being composed of 93% NTOd\_S1 → NTOa\_S1 (Fig. S12(a) and (b)†) with a minor contribution from the digermene  $\sigma$  to  $\sigma^*$  orbitals (4% NTOd\_S1s → NTOa\_S1s; Fig. S12(c) and (d)†). The

**Table 1** Structural and electronic properties of **3**, Ge<sub>2</sub>(SiMe<sub>2</sub><sup>t</sup>Bu)<sub>4</sub>, Ge<sub>2</sub>{CH(SiMe<sub>3</sub>)<sub>2</sub>}<sub>4</sub> and Ge<sub>2</sub>Trip<sub>3</sub>(SiPh<sub>3</sub>)<sup>16,18b,20</sup>

	<i>d</i> (Ge–Ge) (Å)	$\Sigma$ (angles at Ge)	<i>trans</i> -Bending angle, $\theta$ (°)	Inter-planar angle <sup>a</sup> (°)	$\Delta E_{\text{orb}}$ (triplet) kJ mol <sup>–1</sup>	$\Delta E_{\text{orb}}$ (singlet) kJ mol <sup>–1</sup>
Ge <sub>2</sub> (boryl) <sub>2</sub> (Bcat) <sub>2</sub> ( <b>3</b> ) <sup>b</sup>	2.234(1)	359.2(3), 359.2(3)	4.0, 4.0	0	155.4	299.2
	2.235(1)	360.0(3), 360.0(3)	8.5, 8.5	0		
	2.235(1)	360.0(3), 359.9(3)	2.8, 5.3	3.1		
	2.238(1)	359.2(3), 358.2(3)	14.6, 9.3	4.8		
Ge <sub>2</sub> (SiMe <sub>2</sub> <sup>t</sup> Bu) <sub>4</sub> <sup>c</sup>	2.270(1)	360.0(1)	1.3	7.5	139.4	227.9
Ge <sub>2</sub> {CH(SiMe <sub>3</sub> ) <sub>2</sub> } <sub>4</sub> <sup>c</sup>	2.347(2)	348.5	32.8	0	157.0	142.6
Ge <sub>2</sub> Trip <sub>3</sub> (SiPh <sub>3</sub> ) <sup>c</sup>	2.328(1)	345.3(2), 346.5(2)	34.6, 35.1	13.6	159.1	160.5

<sup>a</sup> Defined as the angle between the two least squares GeXX’ planes. <sup>b</sup> The crystal structure of **3** contains four independent molecules in the asymmetric unit. <sup>c</sup> Metrical data taken from current study and from CIFs JORGJ, LIGTAY and CENWAT (CCDC).<sup>16,18b,20</sup>



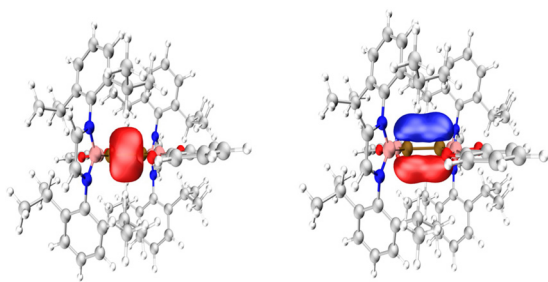


**Fig. 3** Localized molecular orbitals (LMOs) contributing significantly to the electron density (left) at the bond critical point (BCP) and (right) 1 Å above the BCP (and above the  $\text{Ge}_2\text{B}_4$  plane) for  $\text{Ge}_2(\text{boryl})_2(\text{Bcat})_2$ , **3**. The  $\sigma$ -type LMO accounts for 91% of the electron density at the BCP and 48% at 1 Å above the BCP; the  $\pi$ -type LMO accounts for 44% of the electron density at 1 Å above the BCP.

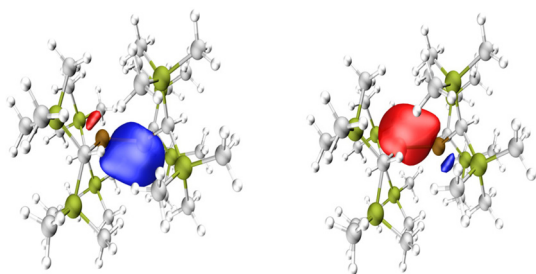


**Fig. 4** Localized molecular orbitals (LMOs) contributing significantly to the electron density at the BCP for  $\text{Ge}_2[\text{CH}(\text{SiMe}_3)_2]_4$  (48% of the electron density, in each case).

higher energy  $S_3$  transition (3.911 eV, 317 nm) also accesses the  $\text{Ge}=\text{Ge}$   $\pi^*$  orbital, in this case from the boryl ligand  $\pi$ -system (99%  $\text{NTOd\_S3} \rightarrow \text{NTOa\_S3}$ ; Fig. S12(e) and (f)†).

Spectroscopic and quantum chemical evidence is therefore consistent with retention of the dimeric structure of **3** in hydrocarbon solution at room temperature. We also investigated whether the speciation of **3** might be temperature dependent. However, while heating a solution in benzene- $d_6$  over a period of 5 days, did lead to the formation of a single major new species, this could be shown by X-ray crystallographic studies to be the unsymmetrical diboron(4) species  $\text{catBB}(\text{NDippCH})_2$  (**4**; Fig. S8†),<sup>22</sup> formed by reductive B–B bond formation. Despite repeated attempts, we were unable to ascertain the nature of the germanium-containing species formed under these conditions – which according to *in situ* NMR measurements (Fig. S7†) is only very sparingly soluble in benzene- $d_6$  solution.

## Conclusions

In conclusion, we have explored a range of synthetic routes to systems of the type  $[\text{Ge}(\text{boryl})_2]_n$ , with the reaction between a dianionic digermanide nucleophile and a boron halide electrophile proving to be the most viable. The tetraboryl digermene so generated is dimeric both in the solid state and in hydrocarbon

solution and features both a planar ‘alkene-like’ geometry for the  $\text{Ge}_2\text{B}_4$  core, and an exceptionally short  $\text{Ge}=\text{Ge}$  double bond. These structural features are consistent with the known electronic properties of the boryl group, and with conceptual fragmentation into two triplet bis(boryl)-germylene fragments.

## Conflicts of interest

There are no conflicts to declare.

## References

† See ESI† for synthetic and characterizing data for **2** and **3**.  
 § See ESI† for details of quantum chemical calculations.

- (a) P. P. Power, *Nature*, 2010, **463**, 171. See also: (b) C. Weetman and S. Inoue, *ChemCatChem*, 2018, **10**, 4213–4228.
- See, for example: (a) Y. Mizuhata, T. Sasamori and N. Tokitoh, *Chem. Rev.*, 2009, **109**, 3479; (b) D. Martin, M. Soleilhavoup and G. Bertrand, *Chem. Sci.*, 2011, **2**, 389; (c) M. Asay, C. Jones and M. Driess, *Chem. Rev.*, 2011, **111**, 354; (d) T. Chu and G. I. Nikonov, *Chem. Rev.*, 2018, **118**, 3608.
- D. Bourissou, O. Guerret, F. P. Gabbaï and G. Bertrand, *Chem. Rev.*, 2000, **100**, 39.
- M. Usher, A. V. Protchenko, A. Rit, J. Campos, E. Kolychev, R. Tirfoin and S. Aldridge, *Chem. – Eur. J.*, 2016, **22**, 11685.
- A. V. Protchenko, K. H. Birjkumar, D. Dange, A. Schwarz, D. Vidovic, C. Jones, N. Kaltsoyannis, P. Mountford and S. Aldridge, *J. Am. Chem. Soc.*, 2012, **134**, 6500.
- A. V. Protchenko, J. I. Bates, L. M. A. Saleh, M. P. Blake, A. D. Schwarz, E. L. Kolychev, A. L. Thompson, C. Jones, P. Mountford and S. Aldridge, *J. Am. Chem. Soc.*, 2016, **138**, 4555.
- (a) P. P. Power, *Chem. Rev.*, 1999, **99**, 3463; (b) R. C. Fischer and P. P. Power, *Chem. Rev.*, 2010, **110**, 3877; (c) F. Hanusch, L. Groll and S. Inoue, *Chem. Sci.*, 2021, **12**, 2001.
- (a) G. Trinquier, J. P. Malrieu and P. Rivière, *J. Am. Chem. Soc.*, 1982, **104**, 4529; (b) G. Trinquier and J. P. Malrieu, *J. Am. Chem. Soc.*, 1987, **109**, 5303; (c) G. Trinquier, *J. Am. Chem. Soc.*, 1990, **112**, 2130; (d) H. B. Wedler, P. Wendelboe and P. P. Power, *Organometallics*, 2018, **37**, 2929.
- A. Rit, J. Campos, H. Niu and S. Aldridge, *Nat. Chem.*, 2016, **8**, 1022.
- Y. Segawa, M. Yamashita and K. Nozaki, *Science*, 2006, **314**, 113.
- X. Zheng, A. E. Crumpton, A. V. Protchenko, A. Heilmann, M. A. Ellwanger and S. Aldridge, *Chem. – Eur. J.*, 2023, **29**, e202203395.
- See, for example: C. Liu and Z.-M. Sun, *Coord. Chem. Rev.*, 2019, **382**, 32.
- L. Pu, A. D. Phillips, A. F. Richards, M. Stender, R. S. Simons, M. M. Olmstead and P. P. Power, *J. Am. Chem. Soc.*, 2003, **125**, 11626.



- 14 B. Cordero, V. Gómez, A. E. Platero-Prats, M. Revés, J. Echeverría, E. Cremades, F. Barragán and S. Alvarez, *Dalton Trans.*, 2008, 2832.
- 15 M. Tian, J. Zhang, L. Guo and C. Cui, *Chem. Sci.*, 2021, **12**, 14635.
- 16 P. B. Hitchcock, M. F. Lappert, S. J. Miles and A. J. Thorne, *J. Chem. Soc., Chem. Commun.*, 1984, 480.
- 17 M. Stender, A. D. Phillips, R. J. Wright and P. P. Power, *Angew. Chem., Int. Ed.*, 2002, **41**, 1785.
- 18 (a) M. Kira, T. Iwamoto, T. Maruyama, C. Kabuto and H. Sakurai, *Organometallics*, 1996, **15**, 3767; (b) T. Iwamoto, J. Okita, N. Yoshida and M. Kira, *Silicon*, 2010, **2**, 209.
- 19 The only comparably short Ge=Ge bonds among non-cyclic systems are those found in two tetraaryl systems: (a) J. T. Snow, S. Murakami, S. Masamune and D. J. Williams, *Tetrahedron Lett.*, 1984, **25**, 4191; (b) H. Schafer, W. Saak and M. Weidenbruch, *Organometallics*, 1999, **18**, 3159.
- 20 L. Klemmer, Y. Kaiser, V. Huch, M. Zimmer and D. Scheschke, *Chem. – Eur. J.*, 2019, **25**, 12187.
- 21 A. Sidiropoulos, C. Jones, A. Stasch, S. Klein and G. Frenking, *Angew. Chem., Int. Ed.*, 2009, **48**, 9701.
- 22 W. Oschmann, C. Borner and C. Kleeberg, *Dalton Trans.*, 2018, **47**, 5318.

